Int. J. Electrochem. Sci., 7 **(2012)** 6406 - 6416

International Journal of
ELECTROCHEMICAL
SCIENCE
www.electrochemsci.org

Ethanol Electrooxidation on PtRh and PtRu Catalytic Surfaces in 0.1 M NaOH

Boguslaw Pierozynski[*]

Department of Chemistry, Faculty of Environmental Protection and Agriculture; University of Warmia and Mazury in Olsztyn, Plac Lodzki 4, 10-957 Olsztyn, Poland
[*]E-mail: bogpierozynski@yahoo.ca

Received: 16 March 2012 / *Accepted:* 2 June 2012 / *Published:* 1 July 2012

This work is concerned with cyclic voltammetric and a.c. impedance spectroscopy investigations of electrooxidation process of ethanol on PtRh and PtRu catalyst materials, conducted in 0.1 M NaOH supporting electrolyte. The kinetics of ethanol oxidation reaction (EOR) were examined in relation to those recently reported for polycrystalline Pt in the same test solution. In addition, significance of temperature dependence of EOR (examined over the temperature range 22-60 ^{o}C) along with that of the process of underpotential deposition (UPD) of H on these two Pt-based catalysts were discussed in detail.

Keywords: Ethanol electrooxidation, EOR, UPD of H, Pt-based catalysts, temperature dependence, impedance spectroscopy

1. INTRODUCTION

Ethanol, due to its high energy-density and non-toxic properties, makes one of the most promising fuels for low-temperature *Proton Exchange Membrane Fuel Cell* (PEMFC) applications. Moreover, C_2H_5OH could be produced from a number of agricultural products and biomass substrates [1-4]. The process of electrooxidation of ethanol on a Pt-based catalyst surface is a multi-step anodic reaction, which could involve formation of numerous, surface-adsorbed reaction intermediates. It is generally acknowledged [2, 5, 6] that following the surface electrosorption step, ethanol molecule could either dissociate to surface-adsorbed CO_{ads} species, or else it could become electrooxidized to form acetaldehyde. In the presence of adsorbed OH_{ads} species, consecutive oxidation steps lead to the formation of CO_2 or CH_3COOH. A number of catalytic materials, including bulk polycrystalline [3] and various single-crystal surfaces of Pt [3, 6-8], PtRu [2, 9], PtRh [2, 5], PtSn [1, 2, 8, 10-12] and

PtPd [4] alloys/co-deposits (usually dispersed on a large surface area carbon substrate) were examined towards their electrochemical behaviour in ethanol oxidation reaction (EOR). Introduction of binary (or ternary) type Pt-derivatives is very important with respect to catalytic effects that certain elements (e.g. Rh, Ru or Pd) might exhibit in order to facilitate the process of CO_{ads} oxidation or the C-C bond breaking for surface-electrosorbed ethanol molecules.

This work is concerned with EOR, carried-out on the selected binary Pt-based catalyst materials; namely, PtRh and PtRu electrodes, in 0.1 M NaOH supporting electrolyte. Kinetic characteristics of this process in relation to those recently reported for polycrystalline Pt were discussed in some detail. Special consideration was given to the phenomenon of underpotential deposition of H, as well as to the temperature-dependence of ethanol oxidation reaction, comparatively with the effects exhibited by polycrystalline Pt in the same test solution.

2. EXPERIMENTAL

2.1. Solutions and solutes, electrochemical cell and electrodes

Solutions were prepared from water produced by means of an 18.2 MΩ Direct-Q3 UV ultra-pure water purification system from Millipore. Aqueous, 0.1 M NaOH solution was prepared from AESAR, 99.996 % NaOH pellets. Ethanol (Stanlab, pure, p.a., Poland) was used to prepare alkaline solutions, at concentrations of 0.25 and 1.0 M C_2H_5OH. All solutions were de-aerated with high-purity argon (Ar 6.0 grade, Linde), prior to conducting electrochemical experiments.

An electrochemical cell made of Pyrex glass was used during the course of this work. The cell comprised three electrodes: a Pt-based alloy working electrode (WE), equipped with flexible adjustment (in a central part), a reversible Pd hydrogen electrode (RHE) as reference and a Pt counter electrode (CE), both in separate compartments. Prior to each series of experiments, the cell was taken apart and soaked in hot sulphuric acid for at least 3 hours. After having been cooled to about 40 ^oC, the cell was thoroughly rinsed with Millipore ultra-pure water.

The palladium hydrogen electrode, acting as a reversible hydrogen electrode (RHE) was used throughout this work. The palladium RHE was made of a coiled Pd wire (0.5 mm diameter, 99.9 % purity, Aldrich) and sealed in soft glass. Before its use, this electrode was cleaned in hot sulphuric acid, followed by cathodic charging with hydrogen in 0.5 M H_2SO_4 (at current, I_c= 10 mA), until H_2 bubbles were clearly observed in the electrolyte. A counter electrode was made of a coiled Pt wire (1.0 mm diameter, 99.9998 % purity, Johnson Matthey, Inc.). Prior to its use, the counter electrode was cleaned in hot sulphuric acid. Pt/Rh alloy wire electrode (Pt90/Rh10, 1 mm diameter, Goodfellow) and PtRu foil (Pt95.2/Ru4.8, 0.05 mm thick, AlfaAesar) material were used as working electrodes for the purpose of this work.

2.2. Electrochemical equipment and procedures

Cyclic voltammograms were recorded at 22 ^oC and over the temperature range 22-60 ^oC, at a sweep-rate of 50 mV s^{-1} by means of the *Solartron* 12,608 W Full Electrochemical System, consisting

of 1260 frequency response analyzer (FRA) and 1287 electrochemical interface (EI). For a.c. impedance measurements, the 1260 FRA generator provided an output signal of 5 mV amplitude and the frequency range was usually swept between $1.0x10^{5}$ and $1.0x10^{-1}$ Hz. The instruments were controlled by *ZPlot 2.9* or *Corrware 2.9* software for Windows (Scribner Associates, Inc.). Presented here impedance results were obtained through selection and analysis of representative series of experimental data. Usually, three impedance measurements were performed at each potential value. The impedance data analysis was conducted with *ZView 2.9* software package, where the spectra were fitted by means of a complex, non-linear, least-squares immitance fitting program, *LEVM 6*, written by Macdonald [13]. Four equivalent circuits for recognized charge-transfer processes, including constant-phase elements (CPEs) to account for distributed capacitance, were employed to analyze the obtained impedance results, as later shown in Figs. 3a to 3d.

3. RESULTS AND DISCUSSION

3.1. Cyclic voltammetry investigations of ethanol electrooxidation reaction

The cyclic voltammetric behaviour of ethanol electrooxidation reaction on PtRu and PtRh alloy electrodes in 0.1 M NaOH (examined at 0.25 and 1.0 M C_2H_5OH) is shown in Figs. 1a and 1b below, respectively. For the PtRu electrode, an oxidation peak (centred at *ca*. 0.83-0.88 V) appears in the CV profile upon an anodic sweep in Fig. 1a. Then, when the CV sweep is reversed towards the H_2 reversible potential, another anodic peak (centred at *ca*. 0.75 V vs. RHE) becomes revealed in the voltammetric profile.

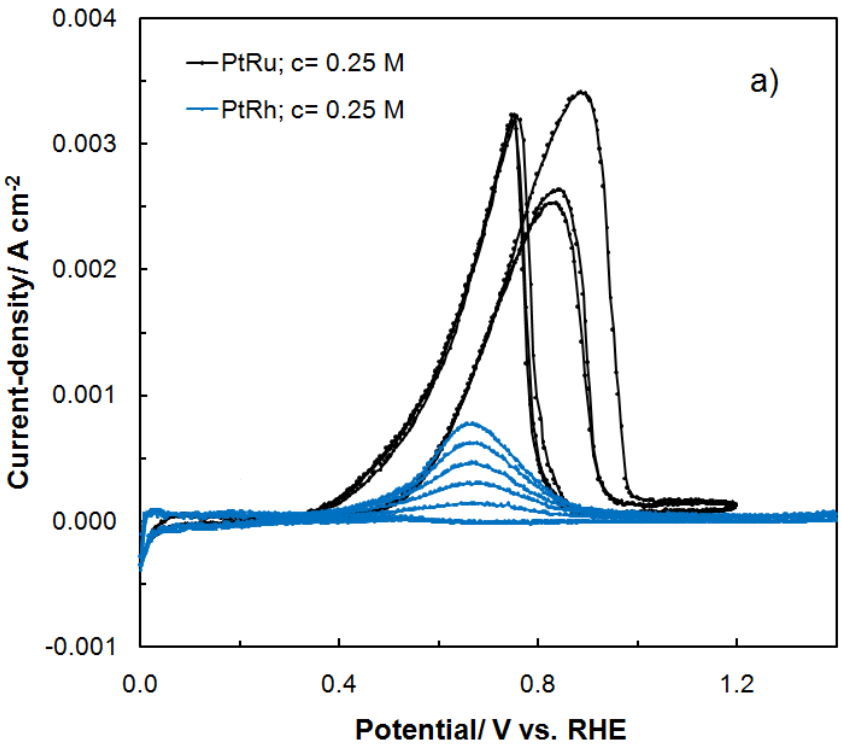

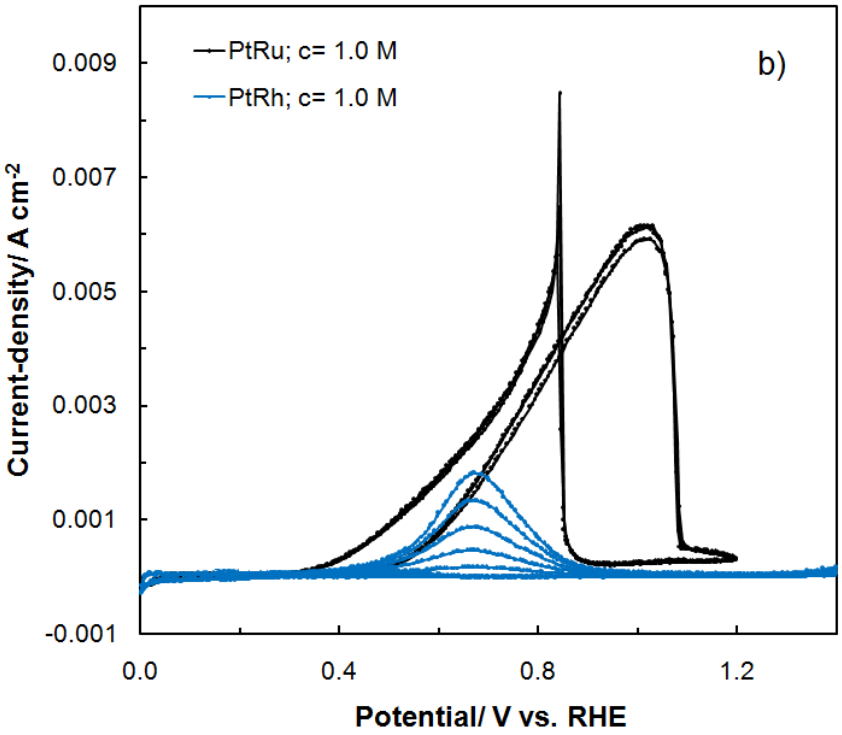

Figure 1. a) Cyclic voltammograms for ethanol electrooxidation on PtRu and PtRh alloy electrodes, carried-out in 0.1 M NaOH, at a sweep-rate of 50 mV s^{-1} and in the presence of 0.25 M C_2H_5OH (three and five consecutive cycles were recorded for each CV run for PtRu and PtRh, respectively); b) As in Fig. 1a, but recorded at 1.0 M C_2H_5OH.

While the latter oxidation peak is usually attributed to the process of oxidation of surface-adsorbed CO_{ads} species, the former one is typically assigned to the formation of acetaldehyde on the catalyst surface [3, 6, 7].

The above-described behaviour is very similar to that recently reported for polycrystalline Pt in 0.1 M NaOH [14]. However, it should be stressed that the EOR carried-out on polycrystalline Pt exhibited considerably larger values of the voltammetric current- densities (compare the respective CV profile in Fig. 1a with that of Fig. 1 in Ref. 14).

On the contrary, a single oxidation peak (centred at about 0.67 V) was recorded for the PtRh electrode (see Fig. 1a again), which implied that the oxidation process was limited to the surface-adsorbed CO_{ads} species, without the formation of acetaldehyde. In addition, the cyclic voltammetry behaviour at the PtRh electrode exhibited dramatically reduced voltammetric current-densities, as compared to those obtained at the PtRu electrode. The latter phenomenon is most likely related to the fact that the presence of Ru [15] element strongly facilitates oxidative desorption of CO_{ads} species (via weakening the Pt-CO bond) from the catalyst surface. In addition, a four-fold increase of ethanol concentration in the supporting electrolyte gave rise to significantly magnified voltammetric current-densities (for both Pt-derived binary catalysts), which could be observed in the corresponding voltammetric profiles of Fig. 1b.

3.2. Electrooxidation of ethanol by a.c. impedance spectroscopy

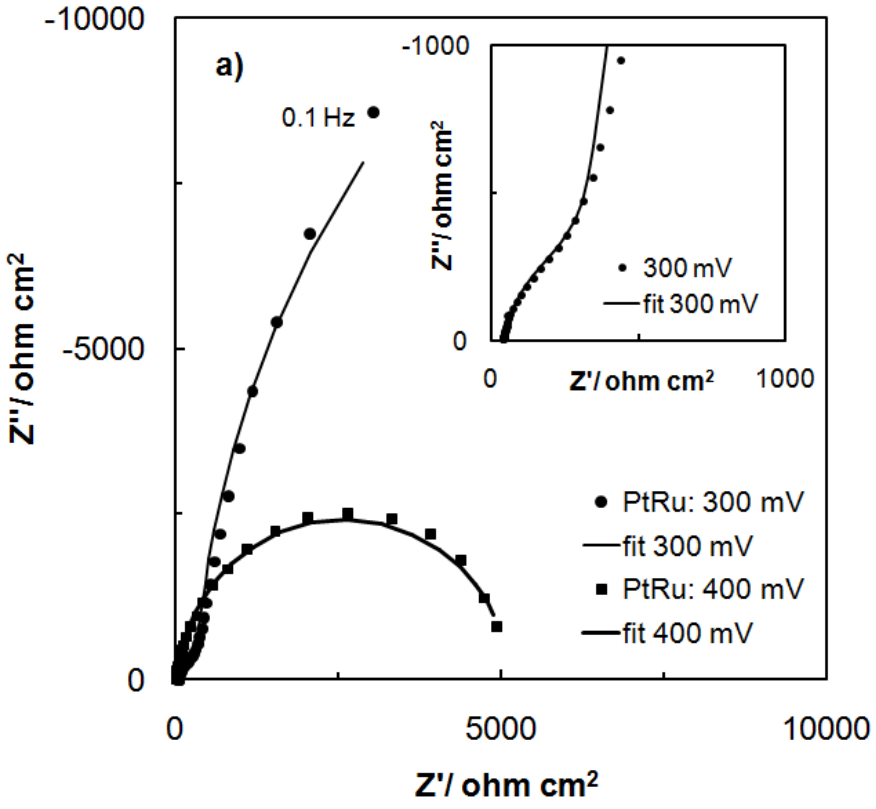

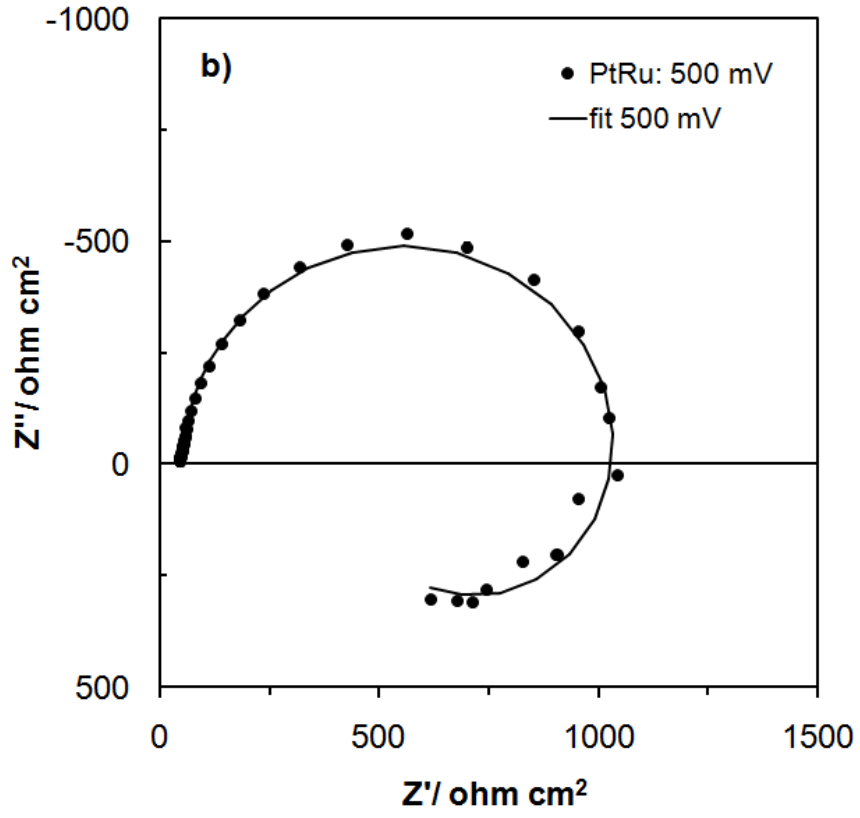

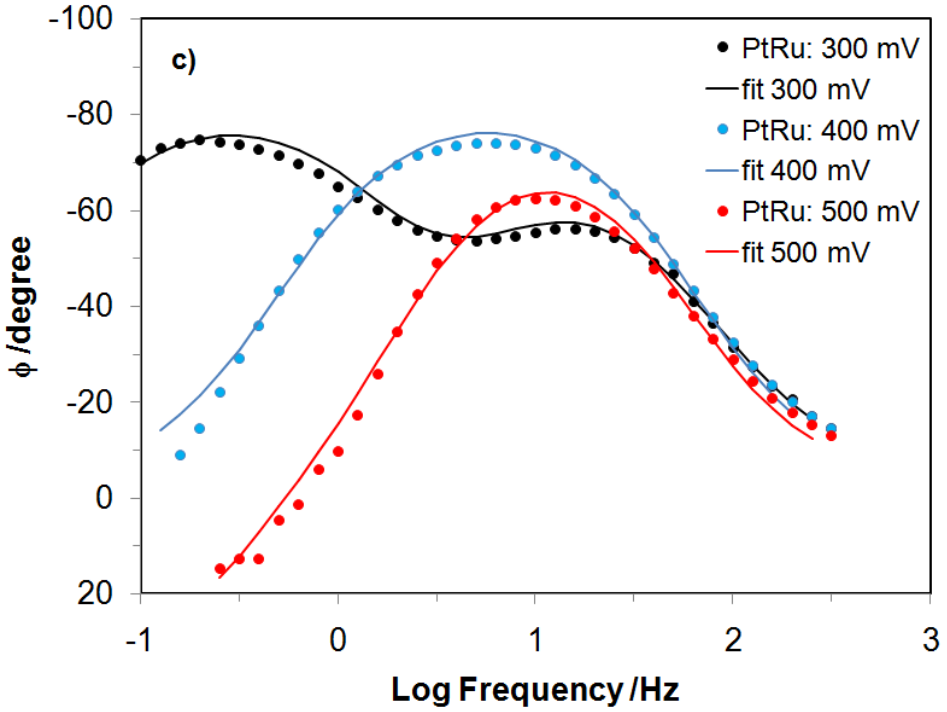

Figure 2. a) Complex-plane impedance plots for PtRu alloy electrode in contact with 0.1 M NaOH, in the presence of 0.25 M C_2H_5OH, recorded at 300 and 400 mV vs. RHE (at 22 ^oC). The solid line corresponds to representation of the data according to equivalent circuits shown in Figs. 3a and 3b; b) As for (a), but recorded at 500 mV in reference to an equivalent circuit shown in Fig. 3d; c) Bode phase-angle plots (other details as in Figs. 2a and 2b above).

The a.c. impedance behaviour of the process of ethanol electrooxidation (in the presence of UPD of H) on PtRu and PtRh alloy catalysts in 0.1 M NaOH (at 0.25 M C_2H_5OH) is presented in Table 1 and Figs. 2a, 2b, and 2c above. For the PtRu electrode, the onset of ethanol oxidation could be observed at 300 mV vs. RHE (Table 1), i.e. over the potential range for UPD of H. The recorded values of the charge-transfer resistance parameter (R_H) for the process of UPD of H in Table 1 were generally in the same order as those recently reported for polycrystalline Pt (under comparable experimental conditions) by Pierozynski in Ref. 14. However, the obtained here rates for UPD of H were significantly slower than those typically reported for Pt catalysts in alkaline supporting electrolyte [16, 17]. Exceedingly high values of the R_H resistance (133.4 and 919.2 Ω cm^2 recorded at 200 and 300 mV, respectively) coincide with very low H adsorption pseudocapacitance (C_{pH}) values (214.0 and 87.0 μF $cm^{-2}s^{\varphi 1-1}$ were recorded at 200, and 300 mV, correspondingly, see Table 1). This behaviour is most likely the result of significant interference from the adsorption of ethanol molecules, which process proceeds in parallel with underpotential deposition of hydrogen.

At 200 mV, the impedance behaviour showed typical features to the process of UPD of H. However, the Nyquist spectrum recorded at 300 mV vs. RHE exhibited two partial, distorted semicircles (see an impedance spectrum obtained at 300 mV along with its high frequency inset in Fig. 2a and the corresponding Bode phase-angle plot in Fig. 2c).

Table 1. Resistance and capacitance parameters for electrooxidation of ethanol (at 0.25 M C_2H_5OH) and UPD of H on PtRu and PtRh alloy electrodes in 0.1 M NaOH (at 22 ^oC), obtained by finding the equivalent circuits which best fitted the impedance data, as shown in Figs. 3a[a] through 3d[d].

E/ mV	R_H/ Ω cm^2	x10^6 C_{pH}/ F $cm^{-2}s^{\varphi 1-1}$	x10^6 C_{dl}/ F $cm^{-2}s^{\varphi 2-1}$	R_{ct}/ Ω cm^2
PtRu				
200[c]	133.4 ± 6.9	214.0 ± 12.6	94.0 ± 3.8	-----
300[a]	919.2 ± 67.1	87.0 ± 5.3	90.4 ± 4.1	33,164 ± 2,643
400[b]	-----	-----	64.8 ± 1.4	5,132 ± 101
	R_o/ Ω cm^2	L/H		
500[d]	585.6 ± 54.4	312.9 ± 14.5	70.3 ± 2.6	1,021 ± 19
600[d]	331.7 ± 36.2	88.8 ± 5.1	39.9 ± 3.9	2,670 ± 245
PtRh				
100[c]	40.7 ± 2.3	230.9 ± 15.4	127.8 ± 16.3	-----
150[c]	434.2 ± 36.0	75.6 ± 5.8	129.2 ± 5.5	-----
200[c]	1,274 ± 103	41.8 ± 2.0	92.5 ± 1.7	-----
300[b]	-----	-----	70.8 ± 0.3	44,235 ± 1,858
400[b]	-----	-----	56.3 ± 0.4	8,961 ± 152
500[b]	-----	-----	111.9 ± 1.0	1,245 ± 11
600[b]	-----	-----	170.8 ± 2.2	7,417 ± 875

The smaller partial semicircle (see inset to Fig. 2a), observed only at high frequencies, corresponds to the process of UPD of H, and a large-diameter partial semicircle, observed throughout the intermediate and low frequency range, is associated with the charge-transfer process (R_{ct}) accompanying ethanol electrooxidation on the PtRu surface. As the UPD of H behaviour is no longer observed at 400 mV, the impedance spectrum at this potential is characterized by the presence of a single partial semicircle, associated with the EOR (see Fig. 2a again). Then, over the potential range 500-600 mV, the corresponding Nyquist impedance spectrum exhibited an inductive loop over the low frequency end (see Fig. 2b). As generally acknowledged [4, 10], the presence of the inductive loop (see the associated inductive resistance, R_o and inductance, L parameters, recorded for the impedance measurements carried-out at 500, and 600 mV in Table 1) is most likely associated with the process of oxidative removal of CO_{ads} species from the catalyst surface, leading simultaneously to the release of the catalyst's active sites. Please note that a remarkable reduction of the inductance (L) parameter (from 312.9 H at 500 mV to 88.8 H at 600 mV) is accompanied by significant diminution of the inductive resistance (R_o) parameter (from 585.6 Ω cm^2 at 500 mV to 331.7 Ω cm^2 at 600 mV). This phenomenon most probably reflects an enhancement of the process of oxidative removal of CO_{ads} species from the PtRu catalyst surface. Simultaneously, minimum of the charge-transfer resistance parameter for ethanol oxidation, R_{ct} = 1,021 Ω cm^2 was recorded at 500 mV, which then significantly increased to reach 2,670 Ω cm^2 at the potential of 600 mV (Table 1).

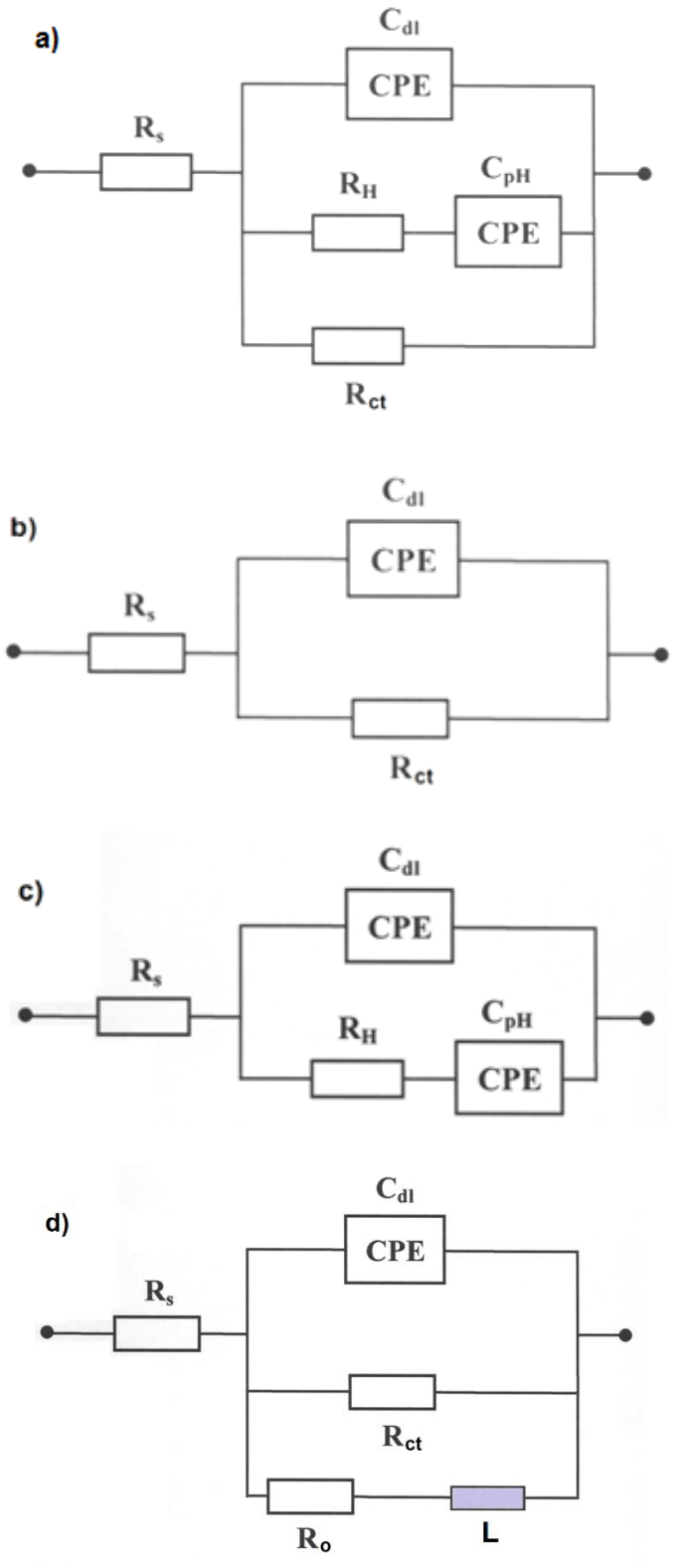

Figure 3. Four equivalent circuits, used for fitting the obtained a.c. impedance spectroscopy data in this work, where: R_s is solution resistance, C_{dl} is double-layer capacitance, R_H and C_{pH} are resistance and pseudocapacitance parameters for the process of UPD of H, R_{ct} is charge-transfer resistance parameter for electrooxidation of ethanol, R_o and L are inductive resistance and inductance parameters, respectively. The circuits include two constant phase elements (CPEs) to account for distributed capacitance.

On the other hand, the recorded double-layer capacitance values (C_{dl}) exhibited substantial oscillations from about 40 to 94 μF $cm^{-2}s^{\varphi 2-1}$. Significantly increased C_{dl} (over that commonly quoted value of 20 μF cm^{-2} for smooth and homogeneous surfaces [18, 19]) implies contribution from surface adsorption processes, involving e.g. reaction intermediates. A deviation from the purely capacitive behaviour requires the use of the CPE components in the equivalent circuits (see Figs. 3a through 3d). This effect corresponds to the so-called dispersion (or distribution) of capacitance and could be caused by increasing surface inhomogeneity, being a result of extensive potentiostatic impedance measurements [20-22]. Here, values of dimensionless parameters φ_1 and φ_2 (for the CPE components in Figs. 3a to 3d, where $0 \leq \varphi \leq 1$) oscillated between 0.81 and 0.98.

Similar impedance behaviour (also with respect to the kinetics of UPD of H) was observed at PtRh catalyst material. However, dramatically rising values of the R_H parameter for the PtRh electrode (compare the recorded R_H values of 1,274 and 133.4 Ω cm^2 at 200 mV for the PtRh, and PtRu catalysts, respectively) suggests that more extensive electrosorption of ethanol molecules takes place on the PtRh surface, as compared to that on the PtRu electrode. Most importantly, for the PtRh material, the EOR exhibited significantly increased R_{ct} values, where the recorded minimum of the R_{ct} (at 500 mV) came to 1,245 Ω cm^2.

Moreover, the recorded at 600 mV value of the charge-transfer resistance parameter increased to 7,417 Ω cm^2, which was about 2.8 times as high as that recorded for the PtRu electrode at analogous potential. In this respect, the impedance-derived data are in good agreement with the conclusions of CV examinations (compare again the cyclic voltammetric profiles for the PtRu and PtRh catalyst materials recorded in Fig. 1a).

Again, the double-layer capacitance parameter for the PtRh electrode showed significant fluctuation and the recorded C_{dl} values (see Table 1 again) considerably exceeded that commonly quoted (20 μF cm^{-2}) value for highly defined and homogeneous surfaces. The recorded dimensionless parameters (φ_1 and φ_2) were between 0.85 and 0.95.

3.3. Temperature-dependence of ethanol electrooxidation reaction

Electrooxidation of ethanol on both examined Pt-based binary catalysts exhibited considerable temperature-dependence. Fig. 4 below presents Arrhenius plots for ethanol oxidation (at 0.25 M C_2H_5OH), carried-out on the PtRu and PtRh alloy electrodes, recorded for the peak anodic current-density potential value, over the temperature range 22-60 ^oC. Thus, an increase of the reaction temperature caused significant amplification of the recorded voltammetric current-densities. Furthermore, apparent activation energies (E_A) for electrooxidation of ethanol on the PtRu and PtRh catalyst materials (derived based on the respective Arrhenius plots) came to 30.8 and 36.0 kJ mol^{-1}, correspondingly.

In fact, these values are significantly higher (compare with 23.5 kJ mol^{-1}) than that recently reported for bulk polycrystalline Pt material in the same test solution [14].

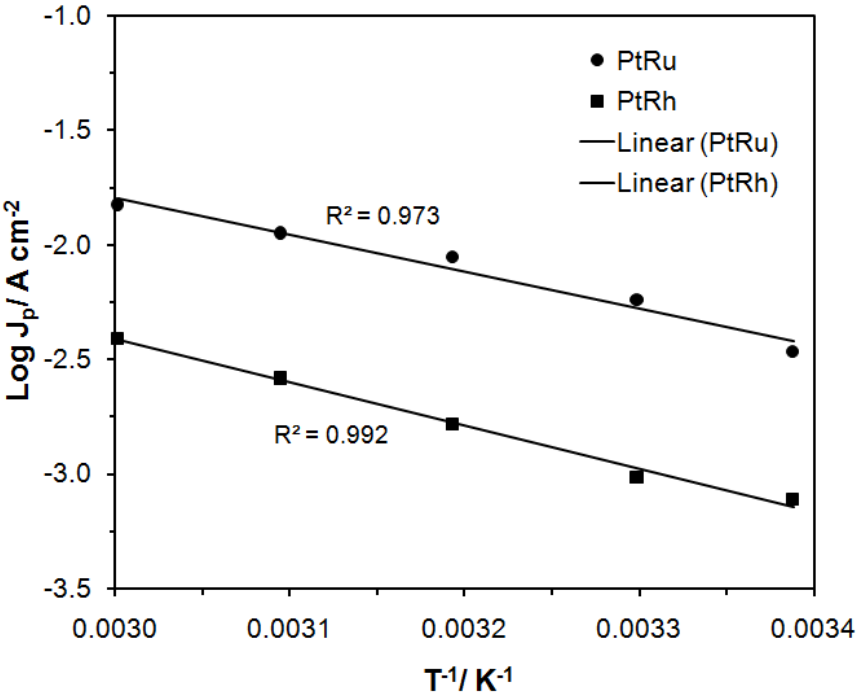

Figure 4. Arrhenius plots for ethanol electrooxidation (at 0.25 M C_2H_5OH) on PtRu and PtRh alloy electrodes in contact with 0.1 M NaOH, recorded for the anodic peak current-density values.

4. CONCLUSIONS

PtRu (Pt95.2/Ru4.8) alloy exhibited significantly enhanced catalytic properties towards ethanol oxidation reaction than PtRh (Pt90/Rh10) material in 0.1 M NaOH supporting electrolyte. The above could be the result of considerably increased rates for oxidative removal of CO_{ads}, which process becomes facilitated in the presence of Ru element. Nevertheless, both examined Pt-based binary alloys exhibited appreciably slower EOR kinetics than those recently reported for bulk polycrystalline Pt material in 0.1 M NaOH.

The presence of ethanol molecules (or reaction intermediates) on the surface of PtRu (or PtRh) catalyst significantly (and adversely) affects the rates for UPD of H (especially evident at PtRh), as compared to those obtained in the absence of ethanol in the supporting electrolyte. In addition, the kinetics of ethanol electrooxidation on PtRu and PtRh alloy materials revealed strong temperature dependence, where the derived apparent energies of activation were considerably higher than that obtained for polycrystalline Pt in the same test solution.

ACKNOWLEDGEMENTS
This work has been financed by the strategic program of the National (Polish) Centre for Research and Development (NCBiR): „Advanced Technologies for Energy Generation. Task 4: Elaboration of Integrated Technologies for the Production of Fuels and Energy from Biomass, Agricultural Waste and other Waste Materials".

References

1. S. Rousseau, C. Coutanceau, C. Lamy and J.M. Leger, *J. Power Sources*, 158 (2006) 18.
2. S.Q. Song, W.J. Zhou, Z.H. Zhou, L.H. Jiang, G.Q. Sun, Q. Xin, V. Leontidis, S. Kontou and P. Tsiakaras, *Int. J. Hydrogen Energy*, 30 (2005) 995.
3. A.A. Abd-El-Latif, E. Mostafa, S. Huxter, G. Attard and H. Baltruschat, *Electrochim. Acta*, 55 (2010) 7951.
4. S.S. Mahapatra, A. Dutta and J. Datta, *Electrochim. Acta*, 55 (2010) 9097.
5. S.S. Gupta and J. Datta, *J. Electroanal. Chem*., 594 (2006) 65.
6. X.H. Xia, H.D. Liess and T. Iwasita, *J. Electroanal. Chem*., 437 (1997) 233.
7. J.F. Gomes, B. Busson, A. Tadjeddine and G. Tremiliosi-Filho, *Electrochim. Acta*, 53 (2008) 6899.
8. A.A. El-Shafei and M. Eiswirth, *Surf. Sci*., 604 (2010) 862.
9. N. Fujiwara, Z. Siroma, S. Yamazaki, T. Ioroi, H. Senoh and K. Yasuda, *J. Power Sources*, 185 (2008) 621.
10. S.S. Gupta, S. Singh and J. Datta, *Mat. Chem. Phys*., 120 (2010) 682.
11. E.E. Switzer, T.S. Olson, A.K. Datye, P. Atanassov, M.R. Hibbs and C.J. Cornelius, *Electrochim. Acta*, 54 (2009) 989.
12. F.C. Simoes, D.M. dos Ajnos, F. Vigier, J.M. Leger, F. Hahn, C. Coutanceau, E.R. Gonzalez, G. Tremiliosi-Filho, A.R. de Andrade, P. Olivi and K.B. Kokoh, *J. Power Sources*, 167 (2007) 1.
13. J. R. Macdonald, *Impedance Spectroscopy, Emphasizing Solid Materials and Systems*, John Wiley & Sons, Inc., New York, (1987).
14. B. Pierozynski, *Int. J. Electrochem. Sci*., 7 (2012) (in press).
15. G. Wu, L. Li and B.Q. Xu, *Electrochim. Acta*, 50 (2004) 1.
16. K.J. Schouten, M.J. van der Niet and M.T. Koper, *Phys. Chem. Chem. Phys*., 12 (2010) 15217.
17. B. Pierozynski and I.M. Kowalski, *J. Electroanal. Chem*., 662 (2011) 432.
18. A. Lasia and A. Rami, *J. Applied Electrochem*., 22 (1992) 376.
19. L. Chen and A. Lasia, *J. Electrochem. Soc*., 138 (1991) 3321.
20. T. Pajkossy, *J. Electroanal. Chem.*, 364 (1994) 111.
21. B.E. Conway in *Impedance Spectroscopy. Theory, Experiment, and Applications*, E. Barsoukov and J. Ross Macdonald (Eds.), Wiley-Interscience, John Wiley & Sons, Inc., Hoboken, N.J., 4.5.3.8 (2005) 494.
22. W.G. Pell, A. Zolfaghari and B.E. Conway, *J. Electroanal. Chem*., 532 (2002) 13.